Published in final edited form as:
Biochim Biophys Acta. 2007 January ; 1772(1): 89–95.

Strain-dependent perinatal lethality of *Ovol1*-deficient mice and identification of *Ovol2* as a downstream target of *Ovol1*

Andy Teng[1], **Mahalakshmi NairJulie Wells**[1,2], **Julia A. Segre**[3], and **Xing Dai**[1,2,*]
1 *Department of Biological Chemistry*

2 *Developmental Biology Center University of California, Irvine, CA 92697*

3 *National Human Genome Research Institute, NIH, 49 Convent Drive, Bethesda, MD 20892*

SUMMARY

Ovol1 encodes a zinc finger transcriptional repressor that is downstream of the LEF1/β-catenin complex, nuclear effectors of canonical Wnt signaling. Previous gene knockout studies performed in a 129Sv x C57BL/6 mixed genetic background revealed that *Ovol1*-deficient mice survive to adulthood but display multiple tissue defects. In this study, we describe a C57BL/6 stain-specific reduction in perinatal survival of *Ovol1* mutant mice. The perinatal lethality is accompanied by kidney epithelial cysts of embryonic onset and delayed skin barrier acquisition. Genetic analysis suggests a partial functional compensation by *Ovol2* for the loss of *Ovol1*. The expression of *Ovol2* was up-regulated in *Ovol1*-deficient epidermis, and Ovol1 represses the activity of *Ovol2* promoter in a DNA binding-dependent manner. Collectively, these studies uncover novel functions of *Ovol1* in mouse development and identify *Ovol2* as a downstream target of Ovol1.

Keywords

Ovol1; *Ovol2*; perinatal lethality; skin barrier; cystic kidney; transcriptional repression

INTRODUCTION

Congenital abnormalities account for 11% of the perinatal death of human infants, a serious health issue especially in developing countries [1]. Understanding the genetic basis and tissue involvement of such abnormalities will ultimately facilitate the development of new and better treatment and management strategies to reduce mortality.

The evolutionarily conserved *ovo* genes encode transcription factors that either activate or repress gene expression and include members that reside downstream of developmental signaling pathways such as Wg/Wnt and BMP/TGF-β [2–4]. A common theme that emerges from functional studies of this gene family in various organisms is a requirement for the development and differentiation of epithelial tissues and germ cells [5–10]. While a single *ovo* gene exists in *Drosophila* and *C. elegans*, three *ovo* paralogs are found in mice, including *Ovol1*, *Ovol2*, and *Ovol3* (also known as *movo*1, *movo*2, and *movo*3, respectively [3]). *Ovol1* is expressed in multiple somatic epithelial tissues including skin and kidney, as well as in the male germinal epithelium [5]. Gene knockout studies revealed a functional requirement for *Ovol1* in these expressing tissues, as mutant mice deficient in *Ovol1* showed ruffled hairs, hyperproliferative epidermis, cystic kidneys, and defective spermatogenesis [5,9,11]. Despite such pleotropic defects, *Ovol1* knockout mice maintained in a 129Sv x C57BL/6 (129 x B6)

*To whom correspondence should be addressed: Department of Biological Chemistry College of Medicine D250 Med Sci I University of California Irvine, CA 92697-1700 Tel: 949-824-3101 Fax: 949-824-2688 E-mail: xdai@uci.edu.

mixed genetic background [5,9] survived to adulthood with no apparent compromise in life-span. *Ovol2* however, is essential for embryonic development, as *Ovol2*-deficient mice die during mid-gestation [10]. Like *Ovol1*, *Ovol2* is also expressed in adult epithelial tissues such as skin and kidney, and in the germinal epithelium of the testis [12].

It is not uncommon that genetic makeup affects the phenotypic manifestation of a particular mutation, and in fact, knockouts of several genes whose mutations affect epithelial development and physiology, including EGFR, keratin 8, and keratin 17, display phenotypic variations in different strain backgrounds [13–18]. Since the initial characterizations of *Ovol1* mutant phenotypes were performed on a 129 x B6 mixed genetic background [5,9], we transferred the *Ovol1* mutant allele into a B6-enriched strain background in order to explore additional functions of *Ovol1* in mammalian development. Our studies now reveal a novel function for *Ovol1* in late embryonic and perinatal survival. Specifically, we show that *Ovol1* mutant animals in the B6-enriched strain background die during late embryonic stages and within the first 2 weeks after birth. This compromised survival is accompanied by kidney cyst formation and delayed skin barrier development in the embryos. We present genetic data suggesting a functional compensation by *Ovol2* for the loss of *Ovol1* in perinatal survival. Finally, we provide molecular evidence demonstrating a direct negative regulation of *Ovol2* expression by Ovol1.

MATERIALS AND METHODS

Mouse breeding and genotyping

Ovol1$^{+/-}$ mice in a 129 x B6 mixed genetic background were backcrossed with B6 mice for 8–10 sequential generations to create “congenic” mice containing the mutant allele (B6-*Ovol1*). B6-*Ovol1*$^{+/-}$ mice were then intercrossed, and offspring (embryos or pups) were genotyped as previously reported [5]. *Ovol1*$^{+/-}$/*Ovol2*$^{+/-}$ double mutant mice were produced by crossing *Ovol1*$^{+/-}$ and *Ovol2*$^{+/-}$ single mutants in a B6-enriched background. The double heterozygotes were then intercrossed to generate compound mutants for analysis.

Histology, barrier assays, and immunohistochemistry

Embryos were fixed in Bouin’s fixative for 12–24 hours at room temperature, processed, and embedded in paraffin. Paraffin sections (5 μm) were prepared and stained with hematoxylin and eosin, and analyzed for morphology. Dye penetration assays were performed using freshly dissected embryos as described [19]. Tails and/or paws were removed for genotyping prior to staining. For immunohistochemistry, embryos were frozen in OCT, and sections (10 μm) were prepared and fixed with 4% paraformaldehyde for 10 minutes, followed by brief washes in PBS. Endogenous peroxidase was quenched by incubation in freshly prepared 3% H_2O_2 solution for 15 minutes. After three 5-minute washes in PBS, sections were subject to immunohistochemical analysis using a polyclonal antibody (1:50) against the full-length Ovol2 protein [20]. Images were acquired using a Nikon Eclipse E600 microscope.

Northern blot analysis

Total RNA was extracted from skin of 2.5-month old wild-type and B6-*Ovol1* mutant mice, and northern blot analysis was performed as described [5] using a 320 bp PCR fragment containing sequences in exons 2 and 3 of *Ovol2* as a cDNA probe.

Electrophoretic mobility shift assay (EMSA)

EMSA assays were performed using different amounts (as indicated in Figure legends) of partially purified recombinant His6-Ovol1 and ~ 20 fmols (~3 x 10^4 cpm) of gel-purified, 5’ ^{32}P-end-labeled double-stranded oligonucleotides. Typically, binding reactions were carried

out in 20 μl volume containing 20 mM Hepes (pH 7.9), 75 mM KCl, 2.5 mM MgCl2, 2 mM DTT, 1 mM EDTA, 12% glycerol and 1 μg of poly (dI-dC) for 30 minutes at room temperature. In competition experiments, a 20- or 100- fold molar excess of unlabeled specific or non-specific competitor was used. The protein-DNA complexes were resolved on 6% non-denaturing polyacrylamide gels and visualized by autoradiography.

Reporter assays

Assays were performed in 293T cells (a human kidney epithelial cell line) as previously described [9]. A typical transfection mixture contained a total of 0.5 μg of plasmids including 50 ng of pGL3-*Ovol2* promoter construct or 10 ng of its mutant derivative with varying amounts of vectors (as indicated in figure legends) expressing Ovol1 [5] or VP16-Ovol1 [11], and 40 ng of a β-actin-β-gal construct. pCB-6 (+) (empty vector containing the CMV promoter) was used as stuffer DNA.

RESULTS

B6-*Ovol1*$^{-/-}$ mutants display perinatal lethality, cystic kidneys with a developmental onset, and delayed skin barrier acquisition

To explore novel functions of *Ovol1* in mouse development, we transferred the previously generated *Ovol1* mutant allele into a C57BL/6 (B6) strain background by 8–10 sequential backcrosses. While in the 129 x B6 mixed background homozygous mutants were born at the expected Mendelian frequency and survived to adulthood [5], intercrosses of *Ovol1*$^{+/-}$ mice enriched with the B6 genome (B6-*Ovol1*$^{+/-}$) yielded fewer than expected *Ovol1*$^{-/-}$ pups when genotyped at postnatal day 14 (P14) (using χ^2 test, p value is <0.005, indicating a <0.5% probability of conforming to the Mendelian law, which predicts a 1:2:1 ratio between +/+:+/−: −/−) (Table 1), implying embryonic or perinatal lethality of homozygous mutants in this new genetic background. To determine the timing of lethality, offspring from such intercrosses were collected at earlier stages and genotyped. Statistically significant deviations from the Mendelian law were observed for newborns and for embryos between the age of E15.5-E18.5, while approximate Mendelian ratios were obtained at and before E14.5 (Table 2). The step-wise decrease in the recovery of homozygous mutants from E15.5 to P14 suggests that death occurred both during late embryogenesis and in the first 2 postnatal weeks. The lethality was completely rescued by a single outcross of the B6-*Ovol1* mice with CD1 mice (Table 1), confirming that the requirement for *Ovol1* in embryonic/perinatal survival is specific to the B6 strain background.

The emergence of a novel lethality phenotype in a B6-enriched background implicates the presence of genetic modifier(s) of *Ovol1* that functions differentially between B6 and 129 or CD1 strains. To address whether *Ovol2* is such a modifier, we genotyped the surviving and perinatal lethal newborns for genetic markers flanking the *Ovol2* locus (D2Mit285 and D2Mit395), but found no linkage between the *Ovol2* locus and survival (data not shown). Therefore, it is unlikely that a B6 allele of *Ovol2* is responsible for the phenotype aggravation of *Ovol1* deletion or a 129 allele of *Ovol2* is providing a protective allele.

Late embryonic and perinatal death can be caused by multiple defects such as developmental abnormalities in kidney (for example [21,22]). Given our previous observation of a mild adult cystic kidney phenotype in the 129 x B6 mixed background [5], we wondered whether B6-*Ovol1* mutant mice developed kidney abnormalities that are more severe or with an earlier age onset. Indeed, many B6-*Ovol1*$^{-/-}$ mutants showed severe unilateral or bilateral cystic kidneys that are apparent to the eye as early as 3 weeks postnatally (Fig. 1A, right), whereas in the original 129 X B6 background such severe cystic kidneys were detected in much older mutant animals and were always unilateral [23]. The penetrance of the defect is also much higher than

the previous background, as most surviving B6-*Ovol1*$^{-/-}$ adults (>90%) displayed enlarged, fluid-filled kidneys. At a histological level, epithelial cysts were apparent as early as E17 in B6-*Ovol1*$^{-/-}$ embryos (Fig. 1B), whereas previously histological kidney anomalies were only detected postnatally [11]. No developmental defects were seen in kidneys from the B6-*Ovol1*$^{+/-}$ mice, and only one out of approximately 40 adult heterozygotes showed a unilateral cystic kidney.

Epidermal development during late embryogenesis gives rise to a functional skin permeability barrier composed of cross-linked proteins and lipids [24]. This barrier is essential for *ex-utero* survival of both mice and humans, as mice born with a defective barrier often die perinatally, whereas the onset of barrier formation in human embryos correlates with the lower age limit at which premature infants survive [24]. The lethality of B6-*Ovol1* mutant mice and the known function of *Ovol1* in developing epidermis [11] prompted us to use dye penetration assays to examine whether B6-*Ovol1* mutants were defective in barrier development [19]. As expected, all wild-type embryos showed precocious sites of dye extrusion at E16.5, and were fully resistant to dye penetration by E17.5 (Fig. 1C, top). In contrast, more than half of the B6-*Ovol1*$^{-/-}$ embryos (n=8) showed no sign of barrier acquisition at E16.5, and all B6-*Ovol1*$^{-/-}$ E17.5 embryos examined (n=5) showed only partial dye extrusion (Fig. 1C, bottom). No apparent dye penetration defects were observed for B6-*Ovol1*$^{-/-}$ embryos at E18.5 and newborn (n=7), or for B6-*Ovol1*$^{+/-}$ embryos at all ages examined (data not shown). These results indicate that B6-*Ovol1* homozygous mutant embryos were delayed in their barrier acquisition by approximately 1 day. Collectively, our findings reveal a previously unrecognized role for *Ovol1* in embryonic/perinatal survival, and in embryonic kidney and skin barrier development.

Ovo12 expression is up-regulated in *Ovol1*-deficient epidermis and *Ovol2* gene dosage affects the frequency of perinatal lethality of *Ovol1*-deficient mice

Functional compensation has been frequently observed between mammalian paralogs, and in such cases the expression of one paralog may be up-regulated when the other is disrupted. The incomplete penetrance of *Ovol1*$^{-/-}$-associated perinatal lethality in the B6-enriched background led us to wonder whether *Ovol2* might be up-regulated to compensate for the loss of *Ovol1*. Northern blot analysis indeed detected significantly higher levels of *Ovol2* transcripts in skin from B6-*Ovol1*$^{-/-}$ mice than that from the wild-type littermates (Fig 2A). We also compared the expression of Ovol2 protein in wild-type and B6-*Ovol1*-deficient skin. In the wild-type epidermis, nuclear Ovol2 protein was detected in the proliferating basal layer, but not in differentiating suprabasal layers that are known to expression Ovol1 [5] (Fig. 2B). In *Ovol1*$^{-/-}$ epidermis however, nuclear Ovol2 protein was produced by not only basal but also suprabasal cells. Together, these results demonstrate that the disruption of *Ovol1* in skin epidermis results in up-regulated expression of *Ovol2*, particularly in the suprabasal layers.

We previously generated *Ovol2*-deficient mice and observed embryonic death before E10.5 [10]. To examine whether *Ovol2* provides a compensatory function for the loss of *Ovol1*, we first generated *Ovol1*$^{+/-}$*Ovol2*$^{+/-}$ compound heterozygotes, which were fertile and displayed no overt phenotype (data not shown). We then intercrossed these mice and genotyped their pups to determine whether a reduction in the gene dosage of *Ovol2* aggravated the postnatal lethality of *Ovol1*$^{-/-}$ mice. Consistent with the reported embryonic lethality caused by *Ovol2* mutation [10], not a single double homozygous mutant was found at P14 among a total of 104 pups that were analyzed (data not shown). Regardless of the *Ovol2* genotype, a less than expected number of *Ovol1*$^{-/-}$ pups were recovered, confirming our conclusion above that *Ovol1* is required for optimum postnatal survival (Table 3). More importantly, a significantly lower-than-expected frequency of *Ovol1*$^{-/-}$*Ovol2*$^{+/-}$ compound mutants was observed, as at a Mendelian ratio, *Ovol1*$^{-/-}$*Ovol2*$^{+/-}$: *Ovol1*$^{-/-}$*Ovol2*$^{+/+}$ should be 2:1 (Table 3; χ^2= 5.08, *p*

value is <0.025, indicating a <2.5% probability of conforming to this ratio). To examine whether the loss of both *Ovol* genes may lead to an earlier embryonic lethality than that are caused by the loss of *Ovol2* alone, we also analyzed embryos from such intercrosses at E8.5. An expected frequency of occurrence was observed for $Ovol1^{-/-}Ovol2^{-/-}$ embryos (5.75 was expected out of 92 embryos analyzed; 5 was observed), and these double mutants are morphologically identical to $Ovol2^{-/-}$ single mutants (data not shown). Collectively, these results indicate that the *Ovol2* gene dosage affects the manifestation of the perinatal lethal phenotype of *Ovol1*-deficient animals, but argue against the notion that *Ovol1* plays a redundant function for *Ovol2* in early embryonic survival.

Molecular evidence that *Ovol2* is a downstream target of Ovol1 transcriptional repression

We have previously reported that Ovol1 is a transcriptional repressor [9,11]. The up-regulation of *Ovol2* expression in $Ovol1^{-/-}$ suprabasal epidermal cells prompted us to test whether *Ovol2* is a target of Ovol1 repression. We examined the sequence of an *Ovol2* promoter fragment (1816 base pairs) that is able to direct active transcription in 293T cells (see below) for putative Ovol1 binding sites. Two CCGTTA elements, known to be the recognition consensus for Ovol1 [11], were found. Oligonucleotides *Ovol2u* and *Ovol2d* containing the upstream and downstream elements, respectively, were tested for Ovol1 binding using EMSA assays. Ovol1 bound to both *Ovol2u* and *Ovol2d*, and the sequence-specificity of the interaction was confirmed by competition by an excess amount of unlabeled specific (lanes 7, 8) but not non-specific (lanes 9, 10) oligonucleotides (Fig. 3A). Furthermore, the identity of the Ovol1-DNA complex was confirmed by the observation of a band supershift when anti-Ovol1 antibody was added to the binding reaction (Fig. 3A, lane 11). Therefore, *Ovol2* promoter contains bona fide Ovol1 binding sites.

We next used reporter assays to examine the effect of Ovol1 on *Ovol2* promoter activity. To do this, we cloned the *Ovol2* promoter fragment upstream of a luciferase reporter gene. Co-transfection with an *Ovol1* expression vector led to a dosage-dependent repression of the activity of this promoter (Fig. 3B). Since repression can sometimes result as an artifact from high levels of protein expression, we turned to test whether VP16-Ovol1, a fusion protein that was shown to activate known Ovol1 target genes [9,11], can activate the *Ovol2* promoter. This fusion protein indeed activated the *Ovol2* promoter in a dosage-dependent manner (Fig. 3C), while VP16 alone had no effect (data not shown). To address whether the observed regulation of *Ovol2* promoter by Ovol1 depends on Ovol1 binding to the promoter, we repeated the experiments, this time using a mutant promoter where both Ovol1 binding sites were removed (by replacing the CCGTTA sequence with a hexamer to which Ovol1 does not bind; [11]). A significant reduction in the degree of activation by VP16-Ovol1 was observed (Fig. 3D), indicating that the maximum effect of Ovol1 on *Ovol2* promoter activity requires Ovol1 binding to these sites. Collectively, these results demonstrate that Ovol1 represses *Ovol2* transcription by binding to its promoter.

DISCUSSION

Our studies have identified a novel function of *Ovol1* in late embryonic/postnatal survival. Furthermore, these results demonstrate that the manifestation of this function is dependent on the strain background where the *Ovol1* mutant alleles reside. There has been an increasing recognition that many Mendelian traits that result in birth defects or adult diseases in mice or human vary in their phenotypic manifestations due to the presence of genetic modifiers [25]. Our work now adds *Ovol1* to the list of genes, including EGFR, keratin 8, and keratin 17, the function of which is influenced by strain-specific modifier(s) [13–18]. Future work to identify such modifier(s) offers exciting opportunities to unravel novel genetic players or pathways that govern developmental processes in which *Ovol1* is required.

What is the underlying basis of perinatal lethality of *Ovol1* knockout mice? While we do not have a definitive answer to this question, we observed defects that are known to associate with perinatal lethality. All mutant embryos examined were able to extrude dye by birth despite a developmental delay in barrier acquisition, making it unlikely that a barrier defect is the underlying cause of lethality. This said, we note that the frequency of a delayed barrier (approximately half) in *Ovol1*$^{-/-}$ embryos is intriguingly similar to that of postnatal lethality of *Ovol1*$^{-/-}$ pups. Furthermore, half of the *Ovol1*$^{-/-}$ pups contain cornified envelops, important constituents of the actual barrier, that show lower resistance to mechanical stress (data not shown). Therefore, we cannot fully exclude the possibility that a compromised barrier under environmental stresses contributes to a certain extent to the reduced *ex utero* survival of *Ovol1* mutant animals. Kidney defect is likely an important contributing factor to lethality. The developmental onset of kidney cysts in B6-*Ovol1*$^{-/-}$ animals is reminiscent of that observed in mice mutant for PKD1, a major target of cystic kidney diseases in humans [22]. PKD1-deficient mice die perinatally, presenting an interesting parallel with the B6-*Ovol1*$^{-/-}$ mice. Most known proteins whose mutations cause cystic renal diseases are localized to the primary cilium of renal tubular epithelial cells [26,27]. Our finding that deletion of Ovol1, a regulatory instead of structural protein, also causes kidney cysts is a first. Our B6-*Ovol1*$^{-/-}$ mice should now provide a useful animal model to study the regulatory mechanisms underlying kidney development and the molecular basis of human cystic kidney diseases.

We used genetic approaches to address the possibility that *Ovol2* provides a compensatory function for the loss of *Ovol1*. We found that mice with only the two *Ovol1* alleles disrupted (*Ovol1*$^{-/-}$*Ovol2*$^{+/+}$) survived better than those with both *Ovol1* alleles as well as a copy of the *Ovol2* allele disrupted (*Ovol1*$^{-/-}$*Ovol2*$^{+/-}$). Taking this result together with our observation of increased *Ovol2* expression in an *Ovol1*-deficient background, we surmise that the elevated expression of *Ovol2* compensates for the loss of *Ovol1*, and that this compensation is insufficient with only one wild-type copy of *Ovol2*. Based on this finding, we predict that a complete penetrance of perinatal lethality and/or additional phenotypes might surface when both alleles of *Ovol2* are deleted in the *Ovol1*-deficient background. Since *Ovol2* homozygous deletion causes embryonic lethality prior to the stage when *Ovol1* function is required, a conditional deletion of *Ovol2* needs to be performed to address this notion.

The existing model suggests that *Ovol1* functions to regulate the transition of epithelial progenitor cells from proliferation to terminal differentiation possibly by regulating the expression of downstream target genes including c-Myc and Id2 [9, 11]. Our in vivo and in vitro studies now add *Ovol2* to the list of Ovol1 downstream targets. Under physiological conditions, *Ovol2* is expressed in the proliferating basal but not differentiating suprabasal cells of the epidermis. This expression pattern is reminiscent of c-Myc and Id2, known positive regulators of proliferation and negative regulators of differentiation. Does *Ovol2* function similarly like c-Myc or Id2 to positively regulate proliferation and negatively regulate terminal differentiation? While this may be the case in normal epidermis, the observed compensation by *Ovol2* for the loss of *Ovol1* suggests that the situation under diseased conditions (e.g., when *Ovol1* is lost) is more complex. Clearly, additional studies are warranted to understand the role of *Ovol2* in epidermal proliferation and differentiation under physiological and pathological conditions.

Acknowledgements

We thank Magid Fallahi and Ming Hu for help with mouse breeding. This work was supported by NIH Grants R01-AR47320 and K02-AR51482 awarded to X. D., and Mahalakshmi Nair was partially supported by an institutional predoctoral NIH Training Program in Developmental Mechanisms Underlying Congenital Defects.

References

1. Sule SS, Onayade AA. Community-based antenatal and perinatal interventions and newborn survival. Niger J Med 2006;15:108–14. [PubMed: 16805163]
2. Kowanetz M, Valcourt U, Bergstrom R, Heldin CH, Moustakas A. Id2 and Id3 define the potency of cell proliferation and differentiation responses to transforming growth factor beta and bone morphogenetic protein. Mol Cell Biol 2004;24:4241–54. [PubMed: 15121845]
3. Li B, Mackay DR, Dai Q, Li TWH, Nair M, Fallahi M, Schonbaum C, Fantes J, Mahowald A, Waterman ML, Fuchs E, Dai X. The LEF1/β-catenin complex activates *movo*1, a mouse homolog of *Drosophila ovo* gene required for epidermal appendage differentiation. Proc Natl Acad Sci USA 2002;99:6064–6069. [PubMed: 11983900]
4. Payre F, Vincent A, Carreno S. ovo/svb integrates Wingless and DER pathways to control epidermis differentiation. Nature 1999;400:271–5. [PubMed: 10421370]
5. Dai X, Schonbaum C, Degenstein L, Bai W, Mahowald A, Fuchs E. The ovo gene required for cuticle formation and oogenesis in flies is involved in hair formation and spermatogenesis in mice. Genes Dev 1998;12:3452–63. [PubMed: 9808631]
6. Johnson AD, Fitzsimmons D, Hagman J, Chamberlin HM. EGL-38 Pax regulates the ovo-related gene lin-48 during Caenorhabditis elegans organ development. Development 2001;128:2857–65. [PubMed: 11532910]
7. Mevel-Ninio M, Terracol R, Salles C, Vincent A, Payre F. ovo, a Drosophila gene required for ovarian development, is specifically expressed in the germline and shares most of its coding sequences with shavenbaby, a gene involved in embryo patterning. Mech Dev 1995;49:83–95. [PubMed: 7748792]
8. Oliver B, Perrimon N, Mahowald AP. The ovo locus is required for sex-specific germ line maintenance in Drosophila. Genes Dev 1987;1:913–23. [PubMed: 3428601]
9. Li B, Nair M, Mackay DR, Bilanchone V, Hu M, Fallahi M, Song H, Dai Q, Cohen PE, Dai X. Ovol1 regulates meiotic pachytene progression during spermatogenesis by repressing Id2 expression. Development 2005;132:1463–73. [PubMed: 15716349]
10. Mackay DR, Hu M, Li B, Rheaume C, Dai X. The mouse Ovol2 gene is required for cranial neural tube development. Dev Biol 2006;291:38–52. [PubMed: 16423343]
11. Nair M, Teng A, Bilanchone V, Agrawal A, Li B, Dai X. Ovol1 regulates the growth arrest of embryonic epidermal progenitor cells and represses c-myc transcription. J Cell Biol 2006;173:253–64. [PubMed: 16636146]
12. Li B, Dai Q, Li L, Nair M, Mackay D, Dai X. Ovol2, a Mammalian Homolog of Drosophila ovo: Gene Structure, Chromosomal Mapping, and Aberrant Expression in Blind-Sterile Mice. Genomics 2002;80:319. [PubMed: 12213202]
13. Threadgill DW, Dlugosz AA, Hansen LA, Tennenbaum T, Lichti U, Yee D, LaMantia C, Mourton T, Herrup K, Harris RC, et al. Targeted disruption of mouse EGF receptor: effect of genetic background on mutant phenotype. Science 1995;269:230–4. [PubMed: 7618084]
14. Sibilia M, Wagner EF. Strain-dependent epithelial defects in mice lacking the EGF receptor. Science 1995;269:234–8. [PubMed: 7618085]
15. Miettinen PJ, Berger JE, Meneses J, Phung Y, Pedersen RA, Werb Z, Derynck R. Epithelial immaturity and multiorgan failure in mice lacking epidermal growth factor receptor. Nature 1995;376:337–41. [PubMed: 7630400]
16. Baribault H, Penner J, Iozzo RV, Wilson-Heiner M. Colorectal hyperplasia and inflammation in keratin 8-deficient FVB/N mice. Genes Dev 1994;8:2964–73. [PubMed: 7528156]
17. Baribault H, Price J, Miyai K, Oshima RG. Mid-gestational lethality in mice lacking keratin 8. Genes Dev 1993;7:1191–202. [PubMed: 7686525]
18. McGowan KM, Tong X, Colucci-Guyon E, Langa F, Babinet C, Coulombe PA. Keratin 17 null mice exhibit age- and strain-dependent alopecia. Genes Dev 2002;16:1412–22. [PubMed: 12050118]
19. Hardman MJ, Sisi P, Banbury DN, Byrne C. Patterned acquisition of skin barrier function during development. Development 1998;125:1541–52. [PubMed: 9502735]
20. Mackay, DR. Ph.D. thesis. University of California; Irvine: 2005.

21. Moser M, Pscherer A, Roth C, Becker J, Mucher G, Zerres K, Dixkens C, Weis J, Guay-Woodford L, Buettner R, Fassler R. Enhanced apoptotic cell death of renal epithelial cells in mice lacking transcription factor AP-2beta. Genes Dev 1997;11:1938–48. [PubMed: 9271117]

22. Lu W, Peissel B, Babakhanlou H, Pavlova A, Geng L, Fan X, Larson C, Brent G, Zhou J. Perinatal lethality with kidney and pancreas defects in mice with a targetted Pkd1 mutation. Nat Genet 1997;17:179–81. [PubMed: 9326937]

23. Dai X, Segre JA. Transcriptional control of epidermal specification and differentiation. Curr Opin Genet Dev 2004;14:485–91. [PubMed: 15380238]

24. Segre J. Complex redundancy to build a simple epidermal permeability barrier. Curr Opin Cell Biol 2003;15:776–82. [PubMed: 14644205]

25. Nadeau JH. Modifier genes in mice and humans. Nat Rev Genet 2001;2:165–74. [PubMed: 11256068]

26. Vogel G. News focus: Betting on cilia. Science 2005;310:216–8. [PubMed: 16223997]

27. Witzgall R. New developments in the field of cystic kidney diseases. Curr Mol Med 2005;5:455–65. [PubMed: 16101475]

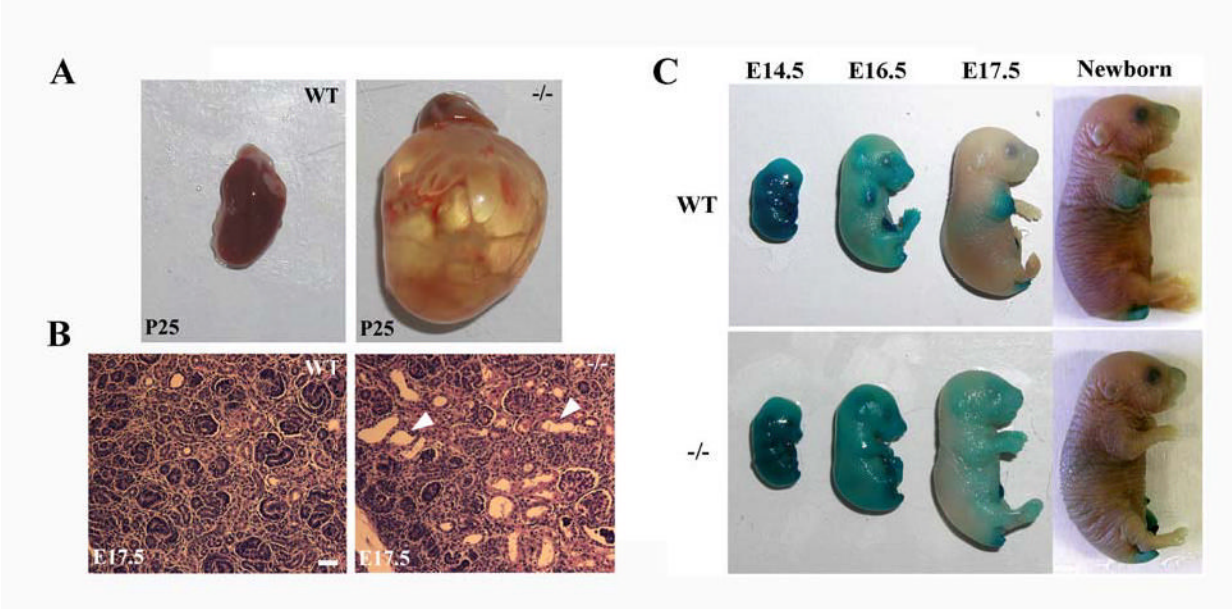

Figure 1. Kidney cysts and delayed barrier acquisition in B6-*Ovol1* mutant mice

(A) Wild-type (left) and mutant (right) kidneys at postnatal day 25. (B) Histology of wild-type (left) and mutant (right) kidneys at E17.5. White arrowheads indicate epithelial cysts in the mutant kidney, while no such cysts were present in the wild-type control littermate. (C) Dye penetration assays of wild-type (top) and mutant (bottom) embryo at the indicated ages. Bar: 20μm in B.

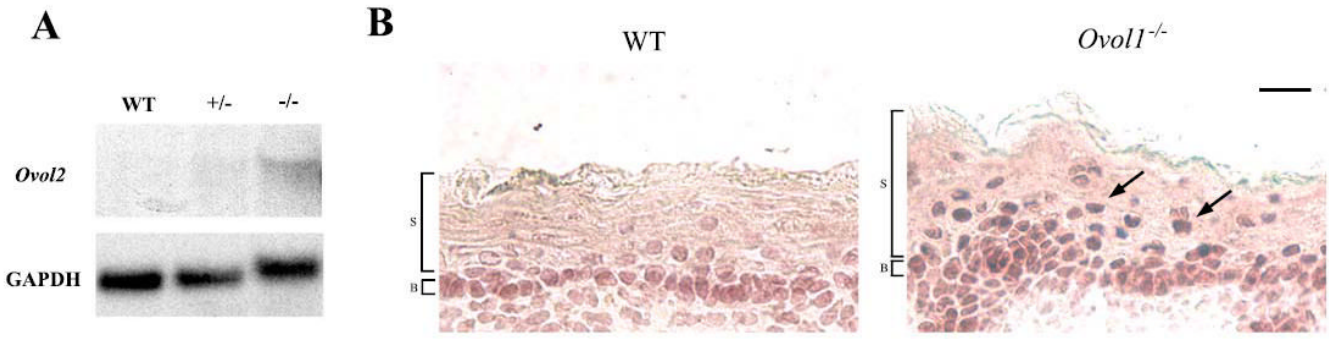

Figure 2. Up-regulated *Ovol2* expression in *Ovol1*-deficient epidermis

(A) Results of northern blot analysis on skin from a surviving 2.5 months-old *Ovol1* $^{-/-}$ mouse and a control littermate. The same blot was stripped and reprobed with GAPDH as a loading control. (B) Results of immunohistochemistry of wild-type (left) and mutant (right) embryonic skin using a rabbit anti-Ovol2 antibody. Arrows indicate the presence of Ovol2 protein in suprabasal cells of the mutant. B, basal; S, suprabasal. Bar: 10 μm in B.

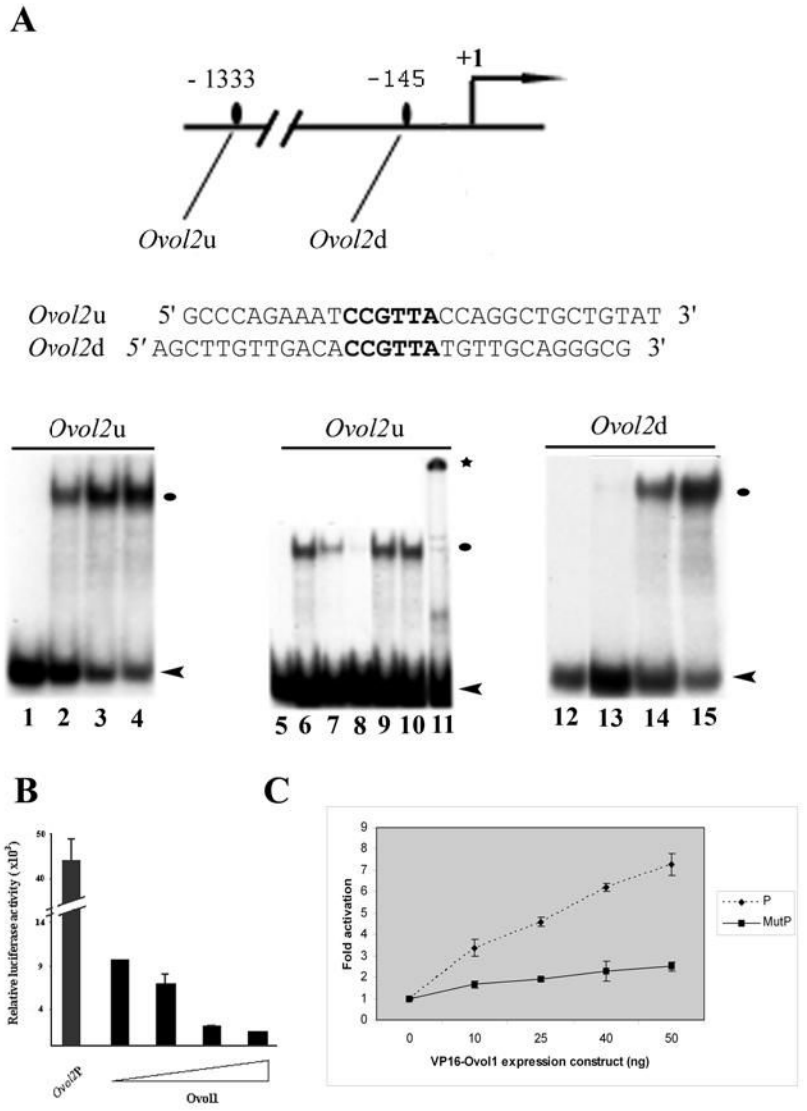

Figure 3. Ovol1 binds to sequences in the *Ovol2* promoter and represses its activity in reporter assays

(A) EMSA assays were carried out with the *Ovol2u* (left) and *Ovol2d* (right) oligonucleotides. Lanes 1, 5, 12: no protein added. Lanes 2, 6, 13: with 0.2 μg recombinant Ovol1. Lanes 3 and 14: with 0.3 μg recombinant Ovol1. Lanes 4 and 15: with 0.5 μg recombinant Ovol1. Lanes 7–11: same as lane 6 but in the presence of a 20- (lanes 7, 9) or 100-fold (lanes 8, 10) excess of unlabeled specific (lanes 7, 8) or non-specific (lanes 9, 10) oligonucleotides, or in the presence of an anti-Ovol1 antibody (lane 11). Black ovals and * indicate the Ovol1-DNA and Ovol1-DNA-antibody complexes, respectively. Arrowheads indicate the position of the free probes. (B–C) Repression (B) and activation (C) of *Ovol2* promoter by Ovol1 (B) and VP16-Ovol1 (C), respectively. The triangle in B indicates increasing concentrations (0, 0.01 μg, 0.02 μg, and 0.05 μg) of the *Ovol1*expression vector. P, wild-type promoter; MutP, mutant promoter in which the Ovol1 binding sites are disrupted. Each bar represents the average of triplicate samples in a single experiment, and results are representative of several independent experiments. Luciferase activities were normalized for transfection efficiency by using a β-actin promoter driving lacZ as an internal control.

Table 1

Genotype distribution of P14 pups from *Ovol1*$^{+/-}$intercrosses in different strain backgrounds

Strain background	Genotype distribution			χ^2	*p*-value
	Ovol1$^{+/+}$	*Ovol1*$^{+/-}$	*Ovol1*$^{-/-}$		
129xB6	**27**	**51**	**25**	**0.1**	**>0.9**
B6 congenic	**145**	**223**	**91**	**13.1**	**<0.005**
CD1xB6	**18**	**41**	**17**	**0.7**	**>0.5**

Table 2

Genotype distribution of embryos and newborns from B6-*Ovol1*$^{+/-}$ intercrosses

Age of offspring	Genotype distribution			χ^2	*p*-value
	Ovol1$^{+/+}$	*Ovol1*$^{+/-}$	*Ovol1*$^{-/-}$		
<E14.5	13	26	14	0.06	>0.9
E15.5–E18.5	144	197	120	12.2	<0.005
P0	117	146	87	14.8	<0.005

Table 3

Genotype distribution of P14 pups from *Ovol1*$^{+/-}$*Ovol2*$^{+/-}$ intercrosses

	Ovol1$^{+/+}$		*Ovol1*$^{+/-}$		*Ovol1*$^{-/-}$	
	Ovol2$^{+/+}$	*Ovol2*$^{+/-}$	*Ovol2*$^{+/+}$	*Ovol2*$^{+/-}$	*Ovol2*$^{+/+}$	*Ovol2*$^{+/-}$
Estimated	**8.7**	**17.4**	**17.4**	**34.8**	**8.7**	**17.4**
Observed	**12**	**20**	**21**	**34**	**9**	**8**
χ^2	**1.64**		**0.76**		**5.08**	
***p*-value**	**>0.1**		**>0.1**		**<0.025**	